ANZIAM J. **62** (2020), 423–445
doi:10.1017/S144618112000005X

ONE-DIMENSIONAL CHAOTIC LAMINAR FLOW WITH COMPETITIVE EXOTHERMIC AND ENDOTHERMIC REACTIONS

S. D. WATT[1], Z. HUANG[1], H. S. SIDHU[1], A. C. MCINTOSH[2] and J. BRINDLEY[3]

(Received 12 April, 2019; accepted 14 January, 2020; first published online 15 April, 2020)

Abstract

We consider the numerical solution of competitive exothermic and endothermic reactions in the presence of a chaotic advection flow. The resulting behaviour is characterized by a strong dependence on the competitive reaction history. The burnt temperature is not immediately connected to simple enthalpy calculations, so there is a subtlety in the interplay between the major parameters, notably the Damköhler number, the ratio of the heats of exothermic and endothermic reactions, as well as the ratio of their respective activation energies. This paper seeks to explore the way these parameters affect the steady states of these reaction fronts and their stability.

2010 *Mathematics subject classification*: 76R50.

Keywords and phrases: chaotic advection, reacting flows, competitive reactions.

1. Introduction

For the first time, we explore in this paper the effects of chaotic advection on the existence and behaviour of combustion fronts driven by exothermal and endothermal reactions, competing for the same reactive fluid fuel. The phenomenology of chaotic advection [1] is a feature of the Lagrangian formulation of the dynamics of fluid flows (in contrast to the much better-known Navier–Stokes formulation). The Lagrangian approach builds on the dynamics of individual fluid particles, which collectively constitute a dynamical system capable of chaotic behaviour [22], under some circumstances. This chaotic advection has profound effects on fluid mixing, and hence on overall reaction rates in reacting flows. It is important to recognize

[1]School of Science, UNSW Canberra, Canberra 2600, ACT, Australia; e-mail: simon.watt@adfa.edu.au, victor7hzj@sina.com, h.sidhu@adfa.edu.au.
[2]School of Chemical and Process Engineering, University of Leeds, Leeds, LS2 9JT, UK; e-mail: andy.c.mcintosh@gmail.com.
[3]Department of Mathematics, University of Leeds, Leeds, LS2 9JT, UK; e-mail: j.brindley@leeds.ac.uk.

that chaotic advection, as defined, is a feature of laminar, essentially low Reynolds number flows, and is not to be confused with turbulent flows, for which both mixing and transport phenomena differ substantially. Important practical examples of chaotic advection range from the biological functioning of living organisms through many fields of science and engineering to our physical environment as influenced by the geophysical fluid [15, 16, 21, 22].

In the work reported here, we have assumed that the mixing and associated reaction chemistry are driven by chaotic advection in the ambient fluid (see Figure 1). In practice, chaotic advection can occur as a result of unsteady stirring of the fluid [22], or, as has been more recently demonstrated, when fluid passes through a random porous solid matrix [5, 12, 13]. In each case, the flow generates regions of convergence (and divergence) on to (away from) singular surfaces in three dimensions, or lines in simplified two-dimensional models (usually identifiable as the stable and unstable manifolds of singularities in the dynamical systems analogy of the real fluid flow). The convergence affects both concentration and temperature fields, and therefore reaction rates, which usually exhibit a streaky spatial variation peaking on the singular surfaces of the chaotic flow [4]. These physical conditions strongly suggest the possible emergence of narrow regions with steep gradients of reactant densities, and temperature (fronts) as a prominent feature.

Most studies of reaction, especially combustion fronts, have assumed a single exothermic reaction, where the phenomenology depends on the reactive–advective–diffusive interplay of reactant and temperature in the Arrhenius model [7]. However, in many practical situations, it is not adequate to lump the chemistry into a single-reaction model, and it is necessary to retain at least two reactions in the lumped model, either both exothermic, or one exothermic and the other endothermic. Practical examples are dominated by solid-state pyrolysis processes, but liquid cases are exemplified by the behaviour of emulsion explosives [14, 21, 23].

In earlier papers we have explored the rich phenomenology of combustion fronts driven by two reactions, either parallel, in which each reaction feeds on its own distinct reactant, or, more interestingly, competitive, in which reactions "compete" for the same fuel [2, 6, 7, 9, 20]. In this earlier research we have assumed that the various constituents and products of the process have been well mixed, with any spatial inhomogeneity confined to thin reactive regions (for example, combustion fronts), within which more specialized modelling (for example, coordinate stretching) is required. However, in many practical situations, the constituents and products of the process have not been well mixed due to chaotic advection and mixing [22]. Therefore, in this paper, we are motivated to adapt to a competitive reactive system, an approach developed for single-step reactions, of a filament model modelling a typical streak as a locally one-dimensional strain flow with convergence towards and divergence along its axis; this is the so-called "Lagrangian filament model" [10, 11].

In this model, advected material lines tend to align along the (longitudinal) stretching direction, while compressing and enhancing gradients in the convergent direction. A reaction–advection–diffusion balance is then possible as a steady state,

https://doi.org/10.1017/S144618112000005X Published online by Cambridge University Press

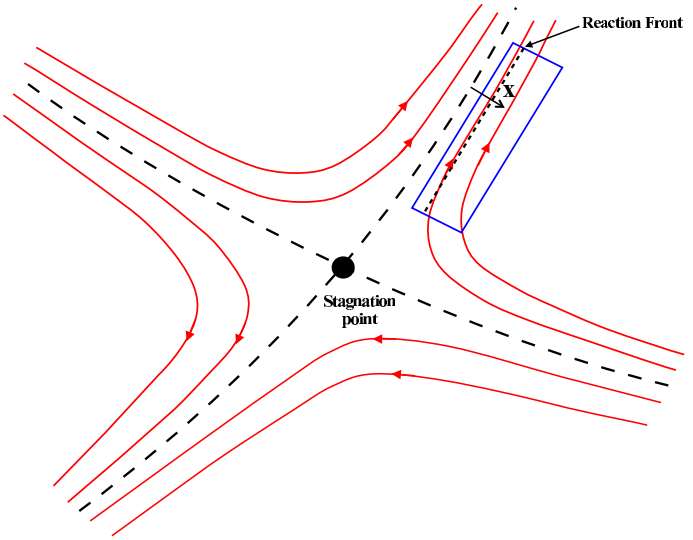

FIGURE 1. The blue box is the region this paper is addressing, where the small advection in the x-direction is illustrated and balanced by diffusion of temperature and species in the same x-direction, and by the reaction term. Colour available online.

in which a stationary reaction front is aligned parallel to the stretching direction and normal to the converging flow. This pseudo one-dimensional configuration is closely analogous to that of the well-known problem of the existence and stability of a combustion front moving with constant speed through a fluid at rest. The essential difference is that the incoming relative fluid speed varies with distance from the front. Thus, we might expect to see a stationary frontal zone at a critical spatial position (see Figure 1), analogous to the critical speed for a travelling combustion wave in fluid at rest. This expectation is borne out by the results of the numerical simulations reported in Sections 4 and 5.

The model chemistry and mathematical expression are presented in Section 2, and a brief discussion of the parameter dependencies in Section 3 is followed by the main results and discussion in Sections 4–6.

2. Mathematical model

We consider the effect of chaotic mixing within a combustion mechanism, in which a fuel (F) undergoes two competitive reactions, one exothermic and another endothermic, with corresponding reaction products (P_1 and P_2), which are assumed to be chemically inert so that they have no effect on physical properties such as fuel density, diffusion coefficient and thermal diffusivity. Symbolically,

$$F \xrightarrow{K_1(T)} P_1 - Q_1(R1) \quad \text{and} \quad F \xrightarrow{K_2(T)} P_2 + Q_2(R2),$$

https://doi.org/10.1017/S144618112000005X Published online by Cambridge University Press

where T is the temperature, K_1 and K_2 are rates of reaction, and Q_1 and Q_2 are enthalpies. Without loss of generality, we assume that $R1$ is endothermic and absorbs heat ($-Q_1 < 0$), and $R2$ is exothermic and releases heat ($Q_2 > 0$).

We will assume Arrhenius kinetics with an ignition temperature of the form

$$K_i(T) = \begin{cases} 0, & T \le T_i, \\ A_i \exp(-E_i/RT), & T > T_i, \end{cases} \tag{2.1}$$

where T is the temperature, $i = 1$ and $i = 2$ denote the endothermic and exothermic reactions, respectively, T_i, A_i and E_i are the ignition temperature, pre-exponential factors and activation energies, respectively, and R is the universal gas constant. By including an ignition temperature (T_i) we avoid the cold boundary problem [24]. For simplicity, we set the ignition temperature $T_1 = T_2 = T_a$, where T_a is the ambient temperature.

Following Kiss et al. [11], here we do not consider the nature of time-dependent fluid flow, but focus on the structures of filaments that arise within the chaotic mixing. We adapt the model presented by Kiss et al. [11] to include a competitive exo-endothermic reaction, namely,

$$\rho c_p\left(\frac{\partial T}{\partial t} - \lambda x\frac{\partial T}{\partial x}\right) = \kappa\frac{\partial^2 T}{\partial x^2} - \rho Q_1 C K_1(T) + \rho Q_2 C K_2(T), \tag{2.2}$$

$$\frac{\partial C}{\partial t} - \lambda x\frac{\partial C}{\partial x} = D\frac{\partial^2 C}{\partial x^2} - CK_1(T) - CK_2(T) \tag{2.3}$$

on $-\infty < x < \infty$, $t > 0$. Here C is the fuel load; x measures distance transverse to the filament; t, ρ and c_p denote the time, density and specific heat, respectively; and κ and D are the thermal conductivity and diffusion coefficient, respectively.

As discussed by Kiss et al. [11], the convective terms in equations (2.2) and (2.3) can be interpreted as advection by a pure strain flow at a constant stretching rate $-\lambda$ (with $\lambda > 0$) along the convergent direction, and we can associate λ with the Lyapunov exponent of the chaotic advection [18].

We assume ambient conditions on the left and right boundaries, namely,

$$T \to T_a, \quad \text{and} \quad C \to C_0 \quad \text{as } |x| \to \infty \ (t > 0),$$

where C_0 denotes the initial fuel load.

From a mathematical viewpoint, it is convenient to consider a dimensionless version of the system (2.2) and (2.3). We therefore introduce the variables

$$u = \frac{RT}{E_2}, \quad c = \frac{C}{C_0}, \quad x' = \sqrt{\frac{\lambda}{D}}x, \quad t' = \lambda t. \tag{2.4}$$

Substituting (2.4) into the systems (2.2) and (2.3) and omitting the primes leads to

$$\frac{\partial u}{\partial t} - x\frac{\partial u}{\partial x} = \mathrm{Le}\,\frac{\partial^2 u}{\partial x^2} - \frac{qr\,\mathrm{Da}}{\Theta}ck_1(u) + \frac{\mathrm{Da}}{\Theta}ck_2(u), \tag{2.5}$$

$$\frac{\partial c}{\partial t} - x\frac{\partial c}{\partial x} = \frac{\partial^2 c}{\partial x^2} - r\,\mathrm{Da}\,ck_1(u) - \mathrm{Da}\,ck_2(u), \tag{2.6}$$

https://doi.org/10.1017/S144618112000005X Published online by Cambridge University Press

where

$$\mathrm{Da} = \frac{A_2}{\lambda}, \quad \mathrm{Le} = \frac{\kappa}{\rho c_p D}, \quad \Theta = \frac{c_p E_2}{C_0 Q_2 R}, \quad q = \frac{Q_1}{Q_2}, \quad r = \frac{A_1}{A_2}. \tag{2.7}$$

We refer to the parameter Da as the Damköhler number, Le as the Lewis number, Θ as the exothermicity parameter and q, r as the ratios of enthalpies and reaction constants, respectively. The temperature dependence of the reaction (2.1) becomes

$$k_1(u) = \begin{cases} 0, & u \le u_a, \\ \exp(-f/u), & u > u_a, \end{cases}$$

$$k_2(u) = \begin{cases} 0, & u \le u_a, \\ \exp(-1/u), & u > u_a, \end{cases}$$

where

$$u_a = \frac{RT_a}{E_2}, \quad f = \frac{E_1}{E_2}. \tag{2.8}$$

We note here that for the case $r = 0$, the system reduces to that studied by Kiss et al. [11], and when $\mathrm{Da} \to \infty$ the system is equivalent to the system of Hmaidi et al. [9] and Sharples et al. [20].

Defining new variables $\bar{u} = \Theta u$, $\bar{u}_a = \Theta u_a$ and dropping the bars when $u \ge u_a$, equations (2.5) and (2.6) can be rewritten as

$$\frac{\partial u}{\partial t} - x\frac{\partial u}{\partial x} = \mathrm{Le}\,\frac{\partial^2 u}{\partial x^2} - qr\,\mathrm{Da}\,c k_1\left(\frac{u}{\Theta}\right) + \mathrm{Da}\,c k_2\left(\frac{u}{\Theta}\right), \tag{2.9}$$

$$\frac{\partial c}{\partial t} - x\frac{\partial c}{\partial x} = \frac{\partial^2 c}{\partial x^2} - r\,\mathrm{Da}\,c k_1\left(\frac{u}{\Theta}\right) - \mathrm{Da}\,c k_2\left(\frac{u}{\Theta}\right). \tag{2.10}$$

The boundary conditions to be applied are

$$u \to u_a, \qquad c \to 1 \quad \text{as } |x| \to \infty. \tag{2.11}$$

The Damköhler number Da relates the advective and chemical time-scales, where a large Damköhler number corresponds to slow stirring or a fast chemical reaction and a small Damköhler number corresponds to fast stirring or a slow chemical reaction. We will show that there is a critical value of the Damköhler number, below which the system (2.9)–(2.11) has only the trivial solution, implying that the stirring is so strong that the flame is quenched by the flow. When the Damköhler number is above the critical value, there is one stable and one unstable steady filament solution. The critical Damköhler number is a saddle-node bifurcation point connecting the stable and unstable solution branch.

3. Qualitative analysis of the differential equation system

It is useful first of all to review the possible phenomenology in the parameter space inhabited by the model defined by the system (2.9)–(2.11). There are six key

https://doi.org/10.1017/S144618112000005X Published online by Cambridge University Press

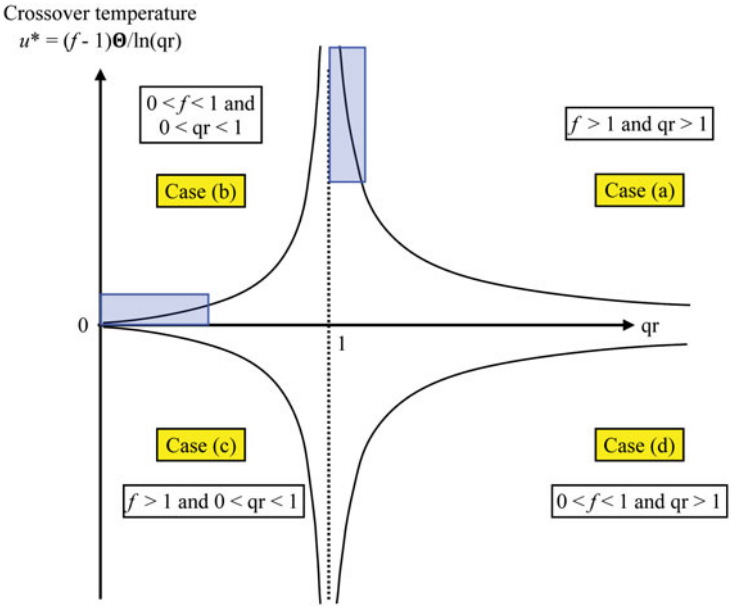

FIGURE 2. Schematic of distinct regions in the parameter space for the balance of reaction terms in the energy equation. This schematic shows the regions which are of primary interest, shaded as blue rectangles. Colour available online.

parameters, as defined in (2.7) and (2.8), and we might expect a rich landscape of phenomena in the various regions of the parameter space. Some narrowing of choice is necessary for progress, and we are initially guided by the division into four regions introduced and fully defined in Figure 2. Specifically, we denote the "crossover temperature" by $u = u^*$, at which the rate of heat released from the exothermic reaction is equal to the rate of heat consumed by the endothermic reaction, that is,

$$u^* = (f - 1)\Theta / \ln(qr).$$

Depending on the reaction parameters, the crossover temperature can be positive or negative. The crossover temperature is positive when either (a) $f > 1$ and $qr > 1$, or (b) $0 < f < 1$ and $0 < qr < 1$. The crossover temperature is negative when either (c) $f > 1$ and $0 < qr < 1$, or (d) $0 < f < 1$ and $qr > 1$. A schematic of these four cases is shown in Figure 2.

Cases (a) and (b) will be explored in Sections 4.1 and 4.2, respectively. When the crossover temperature is negative, one of the reactions will dominate. For case (c), the heat balance is in favour of heat consumption, and the rate of heat consumed by the endothermic reaction is always greater; it implies flame extinction. Gubernov et al. [7] studied case (d).

Gubernov et al. [7] identified endothermic ($R1$) and exothermic ($R2$) dominant regimes in a diffusion-thermal model with a two-step competitive exothermic–

https://doi.org/10.1017/S144618112000005X Published online by Cambridge University Press

endothermic reaction mechanism. When $f \to \infty$ or $qr \to 0$, $R1$ is deactivated and the first reaction terms in equations (2.2) and (2.3) can be omitted. Therefore, for this $R2$-dominant regime, the problem becomes a single-step irreversible exothermic reaction model under the effect of chaotic mixing, which has been studied by Kiss et al. [11]. Thus, the study of this case is not repeated here.

In general, one can formulate the enthalpy equation by eliminating the exothermic reaction term by adding together equations (2.9) and (2.10) so that

$$\frac{\partial(u+c)}{\partial t} - x\frac{\partial(u+c)}{\partial x} = \frac{\partial^2(\mathrm{Le}\,u+c)}{\partial x^2} - (q+1)r\,\mathrm{Da}\,ck_1\left(\frac{\Theta}{u}\right), \tag{3.1}$$

$$\frac{\partial c}{\partial t} - x\frac{\partial c}{\partial x} = \frac{\partial^2 c}{\partial x^2} - r\,\mathrm{Da}\,ck_1\left(\frac{u}{\Theta}\right) - \mathrm{Da}\,ck_2\left(\frac{u}{\Theta}\right). \tag{3.2}$$

We also note that when $f = 1$, the system becomes the single-step model with chaotic mixing and $k_1 = k_2$:

$$\frac{\partial u}{\partial t} - x\frac{\partial u}{\partial x} = \mathrm{Le}\,\frac{\partial^2 u}{\partial x^2} + \mathrm{Da}\,c(1-qr)k_1\left(\frac{u}{\Theta}\right),$$

$$\frac{\partial c}{\partial t} - x\frac{\partial c}{\partial x} = \frac{\partial^2 c}{\partial x^2} - \mathrm{Da}\,c(1+r)k_1\left(\frac{u}{\Theta}\right).$$

Furthermore, note that the problem (2.9)–(2.10) with $f = qr = 1$ has only the trivial solution.

4. Steady-state solutions

Setting the time derivatives in (3.1) and (3.2) to zero yields the steady-state system

$$\mathrm{Le}\,u'' + xu' - qr\,\mathrm{Da}\,ck_1\left(\frac{u}{\Theta}\right) + \mathrm{Da}\,ck_2\left(\frac{u}{\Theta}\right) = 0, \tag{4.1}$$

$$c'' + xc' - r\,\mathrm{Da}\,ck_1\left(\frac{u}{\Theta}\right) - \mathrm{Da}\,ck_2\left(\frac{u}{\Theta}\right) = 0, \tag{4.2}$$

where primes denote differentiation with respect to x. Due to the nature of the advection term xu', the solutions will be symmetric and the boundary conditions become

$$u'(0) = c'(0) = 0, \quad u \to u_a, \quad c \to 1 \quad \text{as } x \to \infty.$$

By adding the two equations together one obtains the steady-state enthalpy and species equations

$$\mathrm{Le}\,u'' + c'' + x(u+c)' - (q+1)r\,\mathrm{Da}\,ck_1\left(\frac{u}{\Theta}\right) = 0, \tag{4.3}$$

$$c'' + xc' - r\,\mathrm{Da}\,ck_1\left(\frac{u}{\Theta}\right) - \mathrm{Da}\,ck_2\left(\frac{u}{\Theta}\right) = 0.$$

The form of equation (4.3) shows that the solution for the temperature necessarily involves the integration of the endothermic term over the whole range of x

https://doi.org/10.1017/S144618112000005X Published online by Cambridge University Press

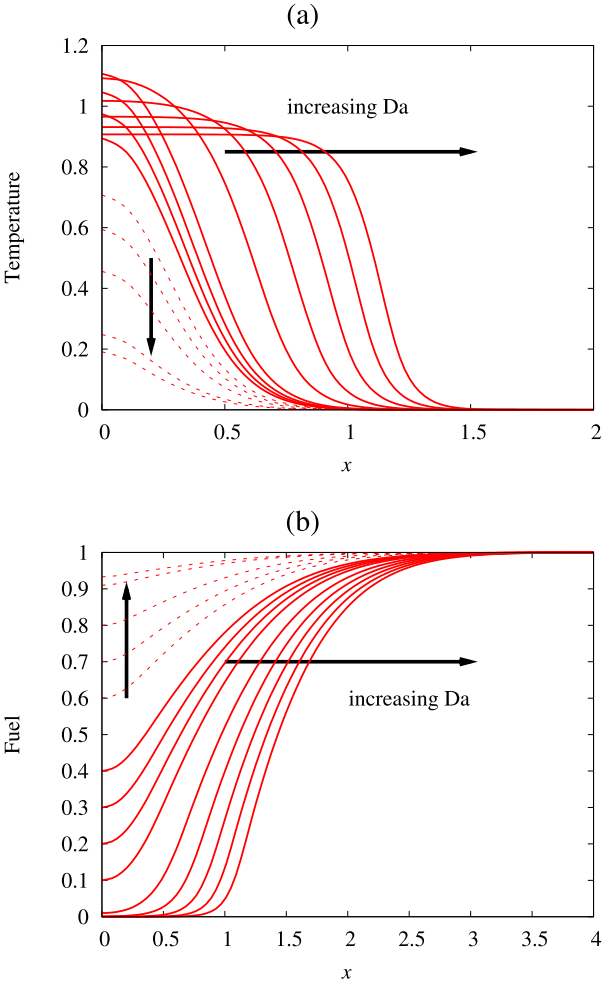

FIGURE 3. (a) Temperature u and (b) concentration c profiles for Le = 0.1 with $q = r = 1$, $f = 2$, $\Theta = 1$ and $u_a = 0.001$.

(or equivalently over the whole history of a typical fluid particle as it travels towards $x = 0$). In other words, the true energy balance involves something more subtle than the schematic used in Figure 2 depending, as it does, on the entire history of the competing reactions.

4.1. Balance between reactions For the purpose of the numerical solution, it is convenient to return to equations (4.1) and (4.2), which were solved using `bvp5c`, a built-in function in MATLAB. The outer boundary conditions were applied at a large value of x, allowing them to be satisfied with sufficient accuracy. The temperature and fuel steady-state profiles are presented in Figures 3, 4 and 5 for different values

https://doi.org/10.1017/S144618112000005X Published online by Cambridge University Press

of the Lewis number, that is, Le = 0.1 (small Lewis number), Le = 1 (Lewis number for gaseous fuels) and Le = 2 (representing porous fuels), respectively, with $\Theta = 1$ and $u_a = 0.001$. The solid lines represent the stable solutions and the dashed lines represent the unstable solutions. Note that, for the most part, the lines are evenly spread with respect to the fuel load at the origin $x = 0$. Figures 4 and 5 show that as Da increases, the burnt temperature (the temperature at $x = 0$) increases for Le ≥ 1. However, Figure 3 shows that as Da increases, the burnt temperature increases at first, but then decreases for Le < 1. Similar behaviour was noticed by Kiss et al. [11]. More generally, we notice that as Da increases, the central temperature in each case approaches a limiting value, but the width of the burnt region increases.

Following the approach of Kiss et al. [11], a measure of the phenomenological behaviour of the system can be given by the integrated quantity

$$I_T(t) = \int_0^\infty (u(x,t) - u_a)\, dx,$$

which can be seen as a proxy for the energy in the system.

Graphs of I_T against Damköhler number are shown in Figure 6 (for Le = 0.1, 0.2, 1 and 2). The solid lines represent the stable solutions and the dashed lines represent the unstable solutions. Here we choose two different values of the ratio of reaction constants, that is, $r = 0$ and $r = 1$. When $r = 0$, the endothermic reaction is deactivated and the problem in (4.1) and (4.2) becomes the one-step reaction with stirring, which has been reported by Kiss et al. [11]. The variation between the results in this work for the case $r = 0$ and the similar problem in [11] arises due to different definitions of the dimensionless temperature. However, the results are in qualitative agreement. When $r = 1$, the endothermic reaction is activated and plays a quenching effect as mentioned by Gubernov et al. [6] and Hamaidi et al. [9]. However, here we are principally concerned with the effect of the strained flow, and Figures 6 and 7 show that there is a critical value of the Damköhler number, $\mathrm{Da}_{\mathrm{crit}}$, above which there are two solutions, one stable and one unstable, and below which the only solution is the trivial solution ($u = u_a$ and $c = 1$). Thus, the transition at the critical Damköhler number can be interpreted as a quenching transition, when the burning of the fuel is not sufficiently fast to compensate for the diluting effect of the stirring, which tends to reduce the temperature of the filament.

Graphs of the burnt temperature u_b against the Damköhler number are shown in Figure 7 for Le = 0.1, 0.2, 1 and 2. For the case of $r = 0$, it can be shown that the burnt temperature approaches $u_a + 1$ for large Damköhler number. For the case of $r = 1$, the burnt temperature approaches a similar limiting value, with a value around 70% of that found when $r = 1$. Another feature of the system is that for Lewis numbers greater than unity, the stable branch monotonically increases to the limit, whereas for Lewis numbers less than unity, the stable branch increases away from the limit, before monotonically decreasing to the limit.

The critical Damköhler number is determined by looking for a nontrivial solution to the homogeneous linear equations that are obtained by making a small perturbation

https://doi.org/10.1017/S144618112000005X Published online by Cambridge University Press

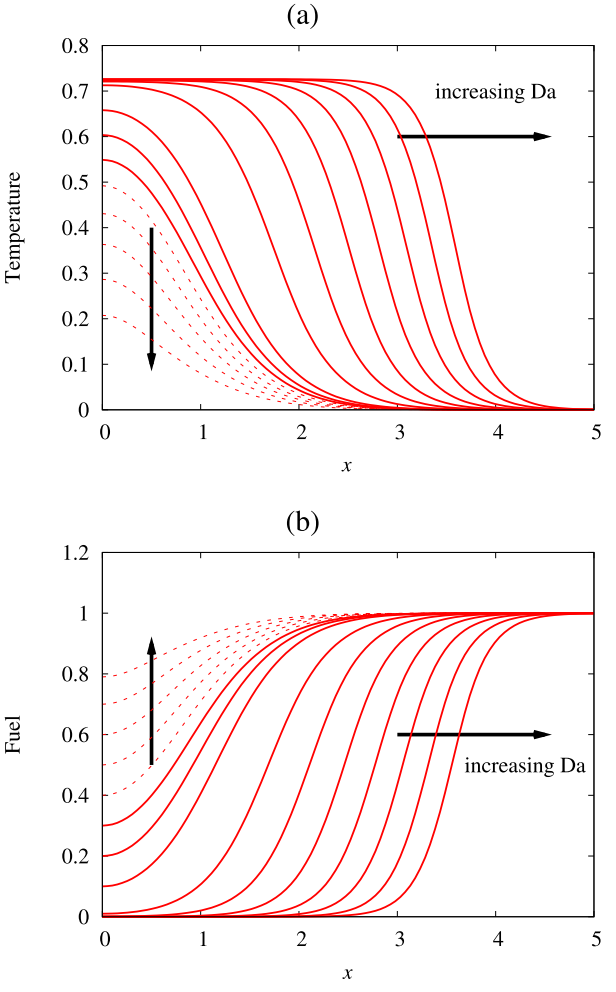

FIGURE 4. (a) Temperature u and (b) concentration c profiles for Le = 1 with $q = r = 1$, $f = 2$, $\Theta = 1$ and $u_a = 0.001$.

to the solutions of equations (4.1) and (4.2). A graph of the critical Damköhler number against the Lewis number is plotted in Figure 8. It is clear that the critical Damköhler number increases with larger Lewis numbers. This implies that the flame is easier to quench by the stirring flow for the combustion with weaker fuel diffusion (larger Lewis numbers).

We next investigate the effect of the endothermic reaction on the problem (4.1)–(4.2) by varying the ratio of enthalpies and reaction rates. A graph of the critical Damköhler number against the ratio of reaction constants is plotted in Figure 9. When the ratio of reaction rates is increased, the endothermic reaction becomes more dominant and the flame is more readily quenched by the flow and so the strain rate

https://doi.org/10.1017/S144618112000005X Published online by Cambridge University Press

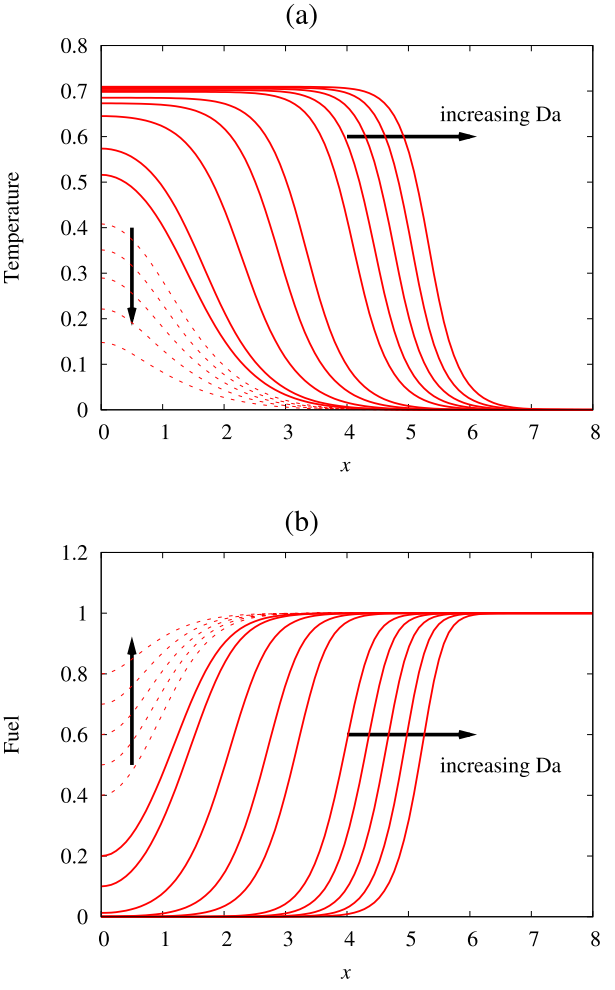

FIGURE 5. (a) Temperature u and (b) concentration c profiles for Le = 2 with $q = r = 1$, $f = 2$, $\Theta = 1$ and $u_a = 0.001$.

should be weaker, which corresponds to a larger Damköhler number. Similarly, when the ratio of enthalpies is increased, the endothermic reaction is taking more heat out of the system and a larger Damköhler number is required.

4.2. Endothermic dominant reactions Until now, we have considered the behaviour where the exothermic reaction has been dominant (case (a), $f > 1$). When the endothermic reaction dominates (case (b), $f < 1$), the regions of the parameter space for which reaction fronts can occur are much more limited, and solutions are more difficult to find numerically, especially for larger exothermicity Θ. As a demonstration that they do occur, however, we present the results for one case in

https://doi.org/10.1017/S144618112000005X Published online by Cambridge University Press

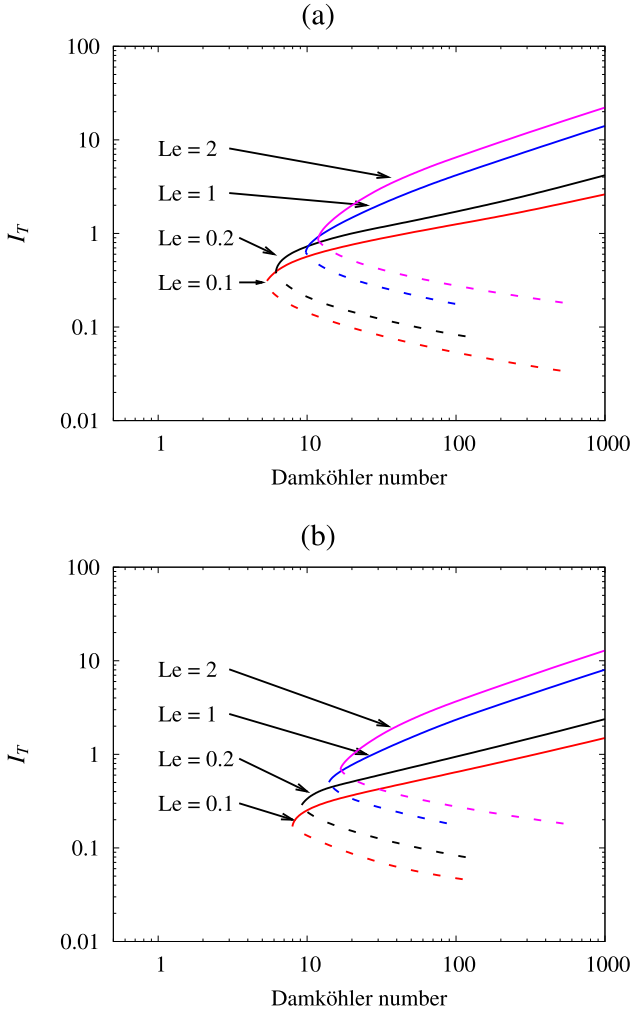

FIGURE 6. Graphs of I_T against the Damköhler number for Le = 0.1, 0.2, 1 and 2 with $q = 1$, $f = 2$ for (*a*) $r = 0$ and (*b*) $r = 1$.

Figure 10. The most striking contrasts with the exothermic cases are to be seen in the lower burnt temperatures and the much larger values of the critical Damköhler number, otherwise the phenomenology is broadly similar. From the figure, the distance between the stable (solid lines) and unstable (dashed lines) solutions is decreasing with increasing Lewis number. This suggests a critical Lewis number where the stable and unstable solution coalesce, leading to an extinction state.

4.3. Solution for large Damköhler number In Figures 3, 4 and 5, for large Damköhler number, we observe that there are two regions of (near) constant temperature and fuel: a central reacted region, where the temperature reaches a burnt

https://doi.org/10.1017/S144618112000005X Published online by Cambridge University Press

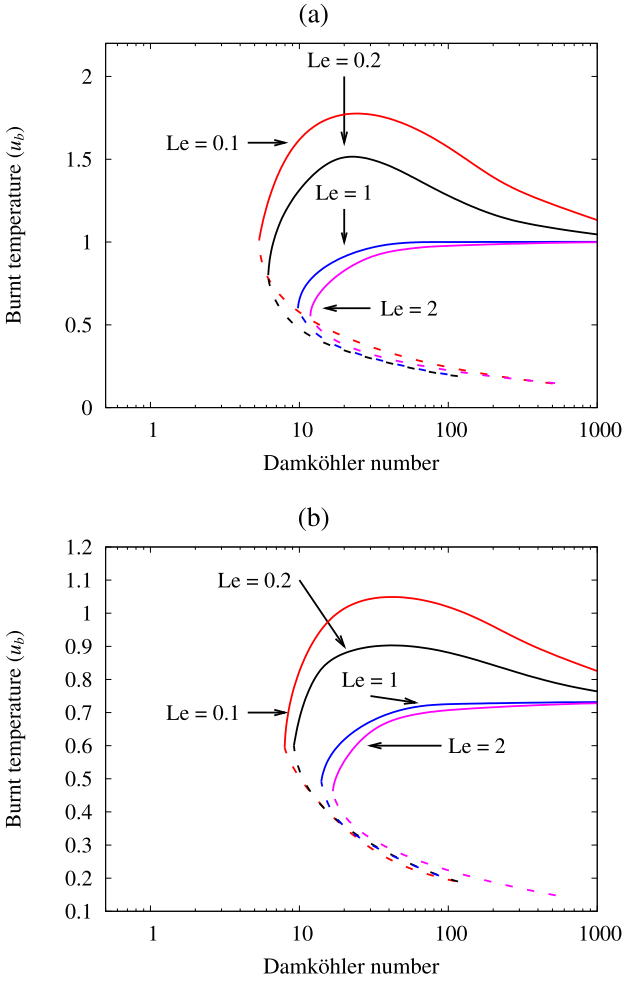

FIGURE 7. Graphs of u_b against the Damköhler number for Le = 0.1, 0.2, 1 and 2 with $q = 1$, $f = 2$ for (a) $r = 0$ and (b) $r = 1$.

temperature and all of the fuel is consumed, and an outer unreacted zone, where the temperature is ambient and the fuel is unconsumed. This suggests that in order to determine the structure of the reaction zone which joins these two regions, we should assume that the zone is centred on $x = x_0(\mathrm{Da})$, and then use a stretched inner coordinate $X \equiv \mathrm{Da}^{1/2}(x - x_0)$ and the series expansions

$$u(X;\mathrm{Da}) = u_0(X) + \mathrm{Da}^{-1}\ u_1(X) + \cdots,$$
$$c(X;\mathrm{Da}) = c_0(X) + \mathrm{Da}^{-1}\ c_1(X) + \cdots,$$

with the maximum temperature $u_c(\mathrm{Da}) = u_c^{(0)} + \mathrm{Da}^{-1}\, u_c^{(1)} + \cdots$ and the location of the reaction front $x_0(\mathrm{Da}) = \mathrm{Da}^{1/2}(a_0 + a_1\,\mathrm{Da}^{-1} + \cdots)$.

https://doi.org/10.1017/S144618112000005X Published online by Cambridge University Press

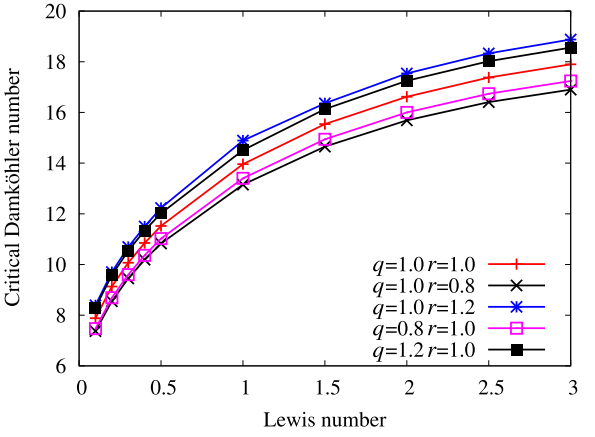

FIGURE 8. A plot of the critical Damköhler number against Lewis number with $f = 2$ and $\Theta = 1$ for various q and r values.

Equations (4.1) and (4.2) at leading order now become

$$\mathrm{Le}\, u_0'' + a_0 u_0' - qrc_0 \exp\Big(-\frac{f\Theta}{u_0}\Big) + c_0 \exp\Big(-\frac{\Theta}{u_0}\Big) = 0, \tag{4.4}$$

$$c_0'' + a_0 c_0' - rc_0 \exp\Big(-\frac{f\Theta}{u_0}\Big) - c_0 \exp\Big(-\frac{\Theta}{u_0}\Big) = 0, \tag{4.5}$$

with boundary conditions

$$u_0 \to u_b^{(0)}, \quad c_0 \to 0 \quad \text{as } X \to -\infty, \quad \text{and} \quad u \to u_a, \quad c_0 \to 1 \quad \text{as } X \to \infty. \tag{4.6}$$

The exothermic reaction can be eliminated by adding these two equations together to give an equation concerning the enthalpy:

$$\mathrm{Le}\ u_0'' + c_0'' + a_0 u_0' + a_0 c_0' - (q+1) r\, c_0\, e^{-f\Theta/u} = 0.$$

Integrating this equation and applying the boundary condition as $X \to \infty$ yields

$$\mathrm{Le}\, u_0' + c_0' + a_0 u_0 + a_0 c_0 - \beta \int_{\infty}^{X} c_0\, e^{-f\Theta/u}\, dX = a_0(1 + u_a), \tag{4.7}$$

where $\beta = (q+1)r$ is the channelling parameter, as given by Hmaidi et al. [9].

It is worth emphasizing again our earlier remark in Section 3 that the essential difficulty of modelling the strained flow considered here is the presence of the integral in equation (4.7), which depends on the detailed history and "memory" of the fluid particles as they approach x_0, preventing any simple expression for the enthalpy evolution in terms of the global parameters. For the case $r = 0$ (and consequently $\beta = 0$), equation (4.7) becomes

$$\mathrm{Le}\ u_0' + c_0' + a_0 u_0 + a_0 c_0 = a_0(1 + u_a).$$

https://doi.org/10.1017/S144618112000005X Published online by Cambridge University Press

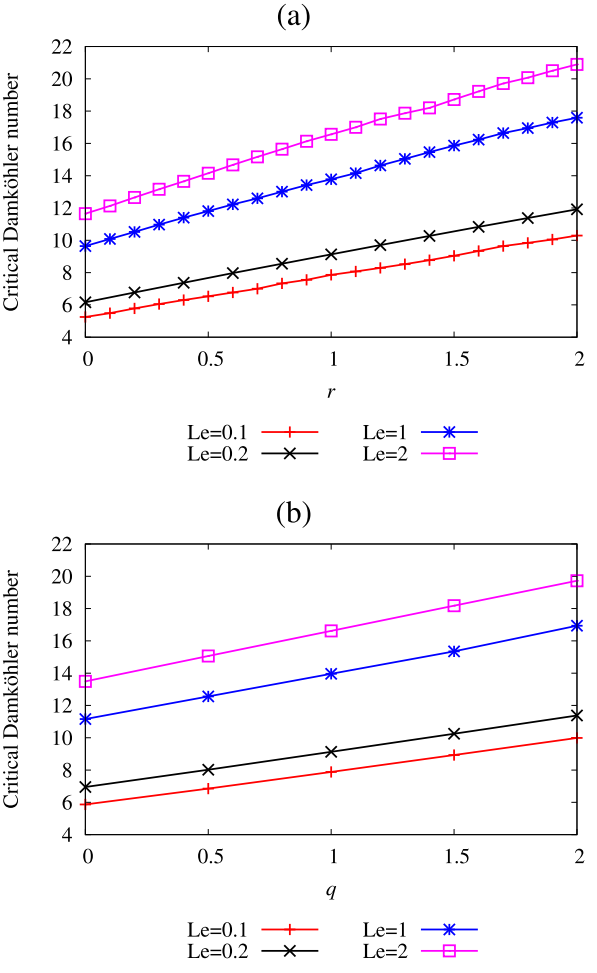

FIGURE 9. A plot of the critical Damköhler number against (a) r and (b) q with $f = 2$ and $\Theta = 1$ for Le = 0.1, 0.2, 1 and 2.

Applying the boundary conditions as $X \to -\infty$,

$$u_0 = u_b^{(0)}, \quad c_0 = 0, \quad u_0' = 0, \quad c_0' = 0,$$

yields the result

$$u_b^{(0)} = 1 + u_a.$$

But for $r \neq 0$, the parameters a_0 and $u_b^{(0)}$ need to be determined by solving equations (4.4) and (4.5), subject to (4.6) (or alternatively (4.7) and either of (4.4) and (4.5)). A graph of a_0 against r and q for different Lewis numbers is shown in Figure 11 for $\Theta = 1$ and $u_a = 0.001$. It is clear that the width of the burnt area, measured by a_0, increases with Lewis number, which is in line with the profiles shown in Figures 3, 4 and 5.

https://doi.org/10.1017/S144618112000005X Published online by Cambridge University Press

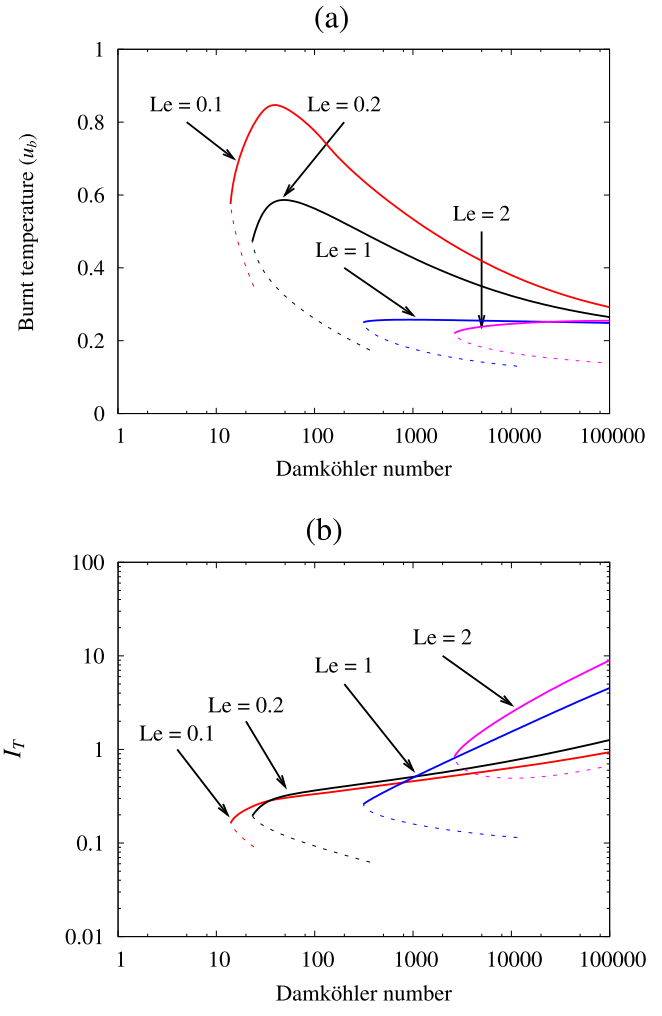

FIGURE 10. A plot of (a) the burnt temperature at $x = 0$ and (b) the total energy I_T for $f = 0.85, q = 0.1$, $r = 1$ and $\Theta = 1$.

In Figure 12, the burnt temperature $u_b^{(0)}$ decreases as the ratio of reaction rates, r, and ratio of enthalpies, q are increased, but is almost independent of the Lewis number, with the curves coalescing. In Figure 13, we see that as Da $\to \infty$, the solution obtained from solving (2.9) and (2.10) approaches the large Damköhler number solution found earlier.

5. Stability of the steady states

We have investigated the stability of the steady states by solving the system of partial differential equations (PDEs) (2.9) and (2.10) together with the boundary

https://doi.org/10.1017/S144618112000005X Published online by Cambridge University Press

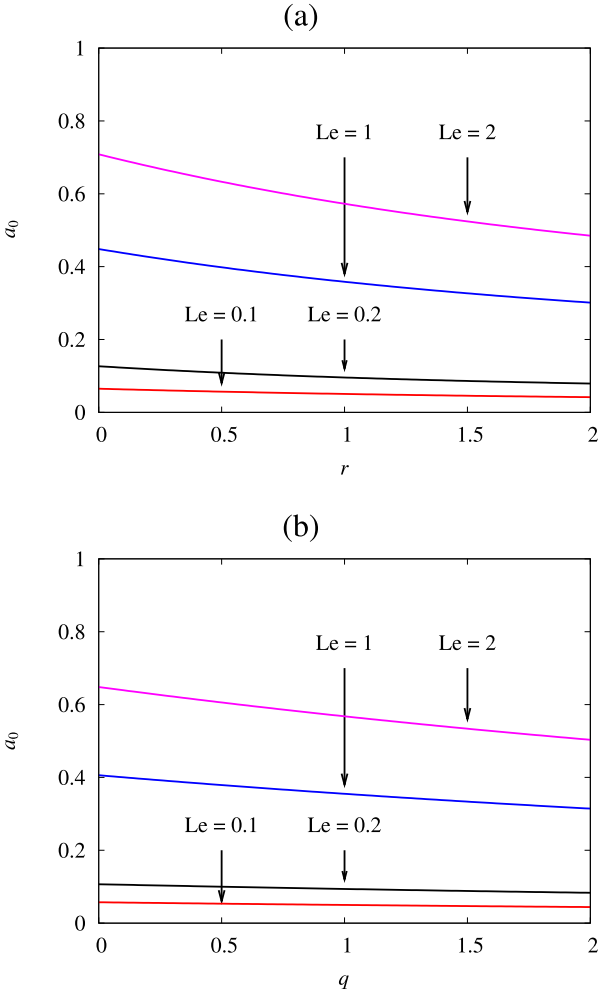

FIGURE 11. The solution of a_0 versus (a) r and (b) q for large Damköhler number with $f = 2$ and $\Theta = 1$ for Le = 0.1, 0.2, 1 and 2.

conditions (2.11). This system was solved by using the method of lines [19] implemented in MATLAB. The method of lines is a standard tool for solving PDEs, which discretizes space to reduce an initial boundary value problem to a system of ordinary differential equations (ODEs) in time. Then a variable time-step approach with time local error control is employed to solve the ODEs.

For the numerical integration of the PDEs (2.9) and (2.10), the initial temperature profile was chosen to be a Gaussian function centred at $x = 0$, which is of the form $u(x, 0) = A \exp(-bx^2)$, imitating an ignition spark. For Damköhler numbers less than the critical value, only trivial solutions were obtained, whereas for Damköhler

https://doi.org/10.1017/S144618112000005X Published online by Cambridge University Press

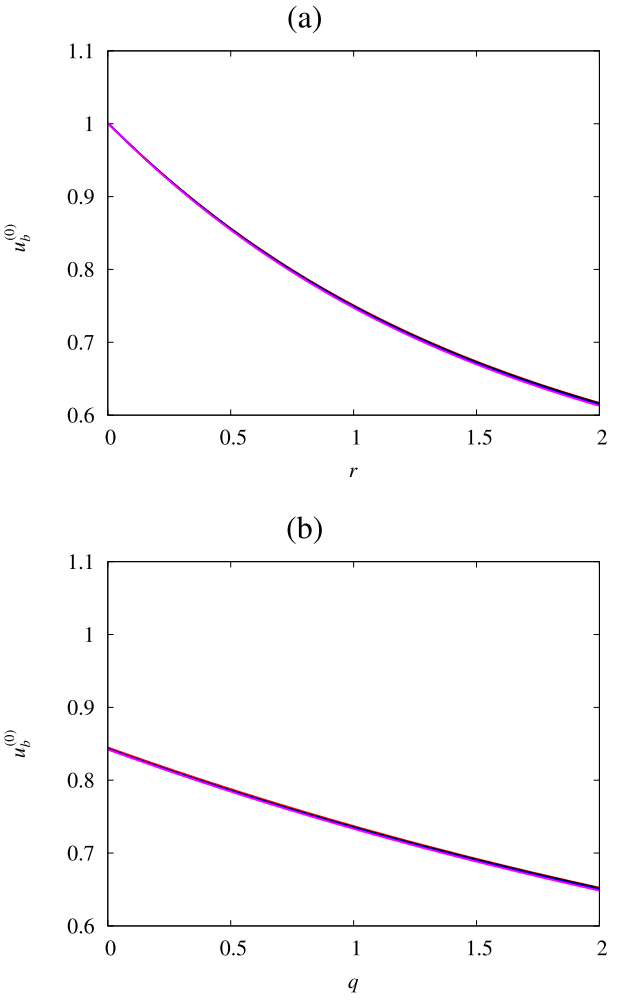

FIGURE 12. A graph of the burnt temperature at the central filament, $u_b^{(0)}$, versus (a) r and (b) q for large Damköhler number with $f = 2$ and $\Theta = 1$ for Le = 0.1, 0.2, 1 and 2.

numbers above the critical value, the upper branch (stable) solutions were obtained, confirming our expectation that the upper branch solutions are stable and the lower branch solutions are unstable.

So far, we have set $\Theta = 1$ in order to stress the effect of chaotic mixing on competitive exothermic–endothermic reactions. We note that without chaotic mixing, the model describing competitive exothermic–endothermic reactions exhibits oscillatory behaviour for large values of the Lewis number and Θ, as shown in [6, 20]. Here we wish to investigate whether or not oscillatory behaviour remains possible with the strained flow represented by equations (2.2) and (2.3). Using FlexPDE^{TM} [17] to

https://doi.org/10.1017/S144618112000005X Published online by Cambridge University Press

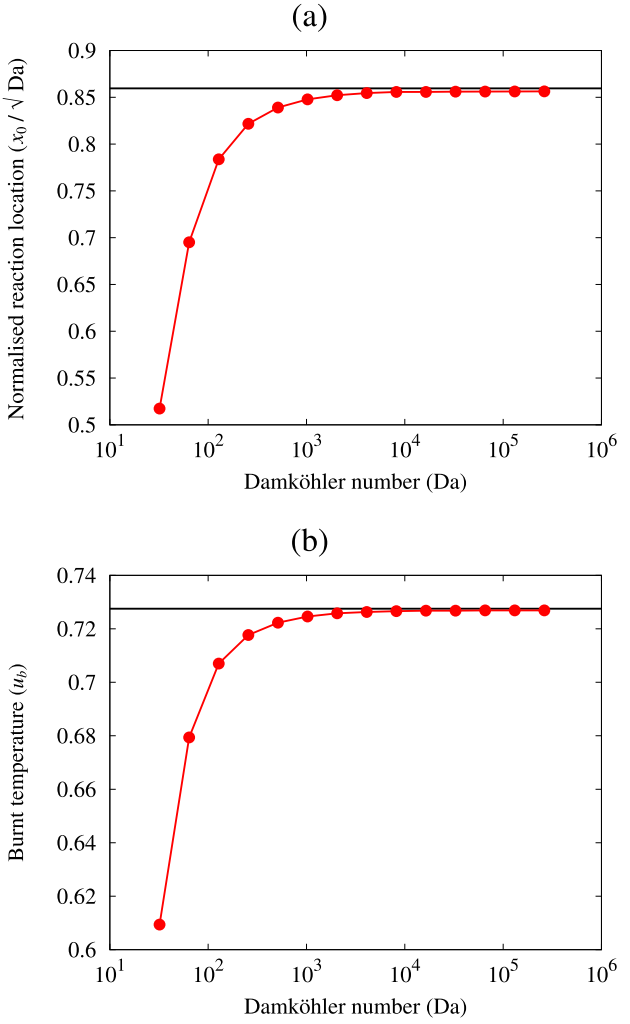

FIGURE 13. Comparison of (a) the filament location (x_0) and (b) the burnt temperature (u_b) as $\text{Da} \to \infty$ (red lines and circles) and the asymptotic results obtained from solving equations (4.4)–(4.6) (horizontal line). Colour available online.

solve the PDEs numerically, we observed oscillatory behaviour for $\text{Le} = 4, \Theta = 8.03$ and $\text{Da} = 10^6$. The time-dependent temperature profile is plotted in Figure 14. Unlike the temperature profiles in Figures 3, 4 and 5, the temperature profiles do not converge over time, but show a periodic deformation.

For $\text{Le} = 4$, $f = 2$, $q = 1$ and $r = 1$, we explored the nature of the solutions for various values of exothermicity Θ and Damköhler number Da. For each value of the Damköhler number, there were two critical exothermicity values. The first was the Hopf point [8], where any value below results in stable steady-state behaviour and

https://doi.org/10.1017/S144618112000005X Published online by Cambridge University Press

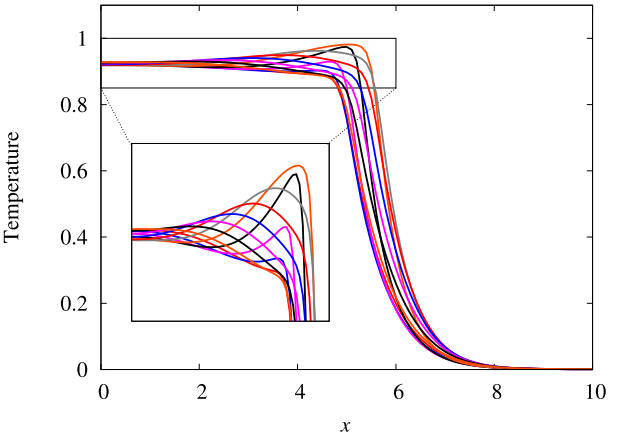

FIGURE 14. Temperature profiles over one period from $t = 50$ to $t = 51.02$ for $\mathrm{Le} = 4, \mathrm{Da} = 10^6, q = 1$, $r = 1, f = 2$ and $\Theta = 8.03$. The different colours represent different points in time. Colour available online.

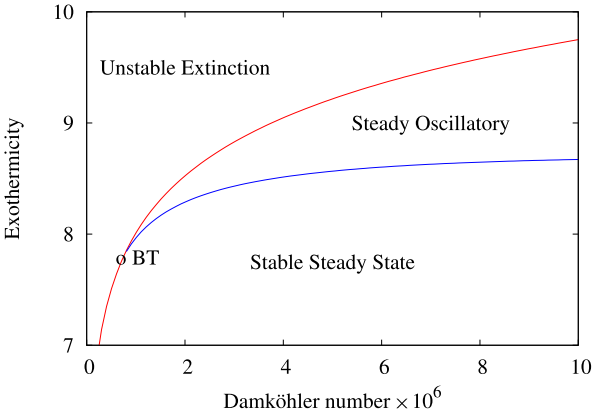

FIGURE 15. Stability diagram showing Hopf and extinction loci and the Bogdanov–Takens bifurcation point (BT) for $\mathrm{Le} = 4, f = 2, q = r = 1$.

above results in oscillatory behaviour. The second was the extinction point, where any value above results in an extinction wave, or quenching, and below results in oscillatory behaviour. It is possible that there is a period-doubling route to extinction, as seen in Sharples et al. [20]; this is not explored here. Figure 15 shows the stability diagram in the $(\mathrm{Da}, \mathrm{Le})$ space for $\mathrm{Le} = 4, f = 2, q = r = 1$. The Hopf curve and extinction curves intersect at the Bogdanov–Takens bifurcation point [8] around $\mathrm{Da} = 7 \times 10^5$ and $\Theta = 7.79$, denoted by BT. As a comparison, Sharples et al. [20] showed that the Hopf point for $\mathrm{Le} = 4, f = 2, q = r = 1$ has exothermicity around 8.93, whereas for the system studied in this paper, the Hopf point is for an exothermicity

https://doi.org/10.1017/S144618112000005X Published online by Cambridge University Press

of about 8.01. The system studied by Sharples et al. [20] is similar to the system studied in this paper, without chaotic mixing. There are some differences in the time and length scales, but the system parameters of exothermicity and the Lewis number quantifying the system behaviour are the same in both systems. Therefore, the addition of the chaotic mixing has some destabilizing effect on the system, when compared to the system without chaotic mixing [20].

6. Summary and discussion

In this paper we have demonstrated, on the basis of a simple strained flow model for an individual streak [5], some of the behaviour to be expected when a multiply-reactive fluid experiences chaotic advection. In particular, we have been concerned with the case where the simplest acceptable lumping approximation of the reaction processes has two components, one exothermic and the other endothermic, each competing for its share of the reactant. Such situations are known to exist in industrial processes, especially production, storage and use of emulsion explosives or high-energy propellants [14, 21, 23], and are believed to be important in geological processes, notably the creation and formation of ore deposits [13]. Some biological processes, especially at the micro or nano level, are also likely candidates.

The multiplicity of the parameter space within which the phenomenology exists has meant that any initial exploration of this kind is partly haphazard, usually guided by existing knowledge of simpler situations, and our case here is no exception. Consequently, we have sought to link our methodologies and results with those for uniform well-mixed flows with competitive reactions (see, for example, [6, 7, 20]) and with those for chaotically advected flows with single reactions [11]. In the first case, we find in Section 5 that the addition of chaotic mixing to the endothermic–exothermic system described by Sharples et al. [20] has a destabilizing effect, in which the stable steady state loses stability at a lower exothermicity. In the second case, we find in Section 4.1 that the addition of an endothermic reaction to the single-step exothermic reaction with chaotic mixing in [11] reduces the allowable strain rate before quenching occurs.

More generally, our numerical results have been consistent with the body of existing work, and suggestive of the regions of parameter space which merit more rigorous examination, through analytical, essentially asymptotic methods as well as numerical modelling. A particular example is the striking dependence of the burnt temperature u_b on the ratio of reaction constants, r, in Figure 12(a), suggesting possible extinction for some finite value of r. Similarly, for the example where the endothermic reaction is dominant, the stable and unstable solutions start to coalesce as the Lewis number increases, also suggesting possible extinction for some finite value of the Lewis number, as shown in Figure 10(a). These results resonate clearly with a much earlier result [3] on combustion fronts with imposed strain, which identified the downstream, burnt temperature as a vital influence on extinction occurrence. The interesting difference (and difficulty) here is of course that the burnt temperature is a derived

https://doi.org/10.1017/S144618112000005X Published online by Cambridge University Press

quantity depending on the time history of the whole process, as expressed through the integral in equation (4.7), which measures the amount of fuel "stolen" by the endothermic reaction. The burnt temperature is not immediately connected to simple enthalpy calculations. Rather, for each set of parameter values, there is a subtle effect of competitive reaction history which determines the final outcome.

Further work along the lines indicated above is currently in hand, and will be reported elsewhere in due course.

References

[1] H. Aref, "Stirring by chaotic advection", *J. Fluid Mech.* **143** (1984) 1–21; doi:10.1017/S0022112084001233.

[2] R. Ball, A. C. McIntosh and J. Brindley, "Thermokinetic models for simultaneous reactions: a comparative study", *Combust. Theory Model.* **3** (1999) 447–468; doi:10.1088/1364-7830/3/3/302.

[3] J. Buckmaster and D. Mikolaitis, "The premixed flame in a counterflow", *Comb. Flame* **47** (1982) 191–204; doi:10.1016/0010-2180(82)90100-6.

[4] M. J. Clifford, S. M. Cox and E. P. L. Robert, "Lamellar modelling of reaction, diffusion and mixing in a two-dimensional flow", *Chem. Engng J.* **71** (1998) 49–56; doi:10.1016/S1385-8947(98)00107-7.

[5] P. de Anna, M. Dentz, A. Tartakovsky and T. Le Borgne, "The filamentary structure of mixing fronts and its control on reaction kinetics in porous media flows", *Geophys. Res. Lett.* **41** (2014) 4586–4593; doi:10.1002/2014GL060068.

[6] V. V. Gubernov, A. V. Kolobov, A. A. Polezhaev, H. S. Sidhu, A. C. McIntosh and J. Brindley, "Stabilization of combustion wave through the competitive endothermic reaction", *Proc. Roy. Soc. Lond.* A **471**(2180) (2015) 1–12; doi:10.1098/rspa.2015.0293.

[7] V. V. Gubernov, J. J. Sharples, H. S. Sidhu, A. C. McIntosh and J. Brindley, "Properties of combustion waves in the model with competitive exo- and endothermic reactions", *J. Math. Chem.* **50** (2012) 2130–2140; doi:10.1007/s10910-012-0021-y.

[8] J. Guckenheimer and P. J. Holmes, *Nonlinear oscillations, dynamical systems, and bifurcations of vector fields* (Springer, New York, 1983); doi:10.1007/978-1-4612-1140-2.

[9] A. Hmaidi, A. C. McIntosh and J. Brindley, "A mathematical model of hotspot condensed phase ignition in the presence of a competitive endothermic reaction", *Combust. Theory Model.* **14** (2010) 893–920; doi:10.1080/13647830.2010.519050.

[10] I. Z. Kiss, J. H. Merkin and Z. Neufeld, "Homogenization induced by chaotic mixing and diffusion in an oscillatory chemical reaction", *Phys. Rev.* E **70** (2004) 026216–1026216–11; doi:10.1103/PhysRevE.70.026216.

[11] I. Z. Kiss, J. H. Merkin, S. K. Scott, P. L. Simon, S. Kalliadasis and Z. Neufeld, "The structure of flame filaments in chaotic flows", *Physica* D **176** (2003) 67–81; doi:10.1016/S0167-2789(02)00741-8.

[12] T. Le Borgne, M. Dentz and E. Villermaux, "Stretching, coalescence and mixing in porous media", *Phys. Rev. Lett.* **110** (2013) 204501-1–204501-5; doi:10.1103/PhysRevLett.110.204501.

[13] D. R. Lester, G. Metcalfe and M. G. Trefry, "Is chaotic advection inherent to porous media flow?", *Phys. Rev. Lett.* **111** (2013) 174101-1–174101-5; doi:10.1103/PhysRevLett.111.174101.

[14] G. B. Manelis, G. M. Nazin, Yu. I. Rubtsov and V. A. Strunin, *Thermal decomposition and combustion of explosives and propellants* (Taylor & Francis, London, 2003); doi:10.1201/9781482288261.

[15] Z. Neufeld, "Excitable media in a chaotic flow", *Phys. Rev. Lett.* **87** (2001) 108301; doi:10.1103/PhysRevLett.87.108301.

[16] Z. Neufeld, P. H. Haynes, V. Garcon and J. Sudre, "Ocean fertilization experiments may initiate large scale phytoplankton bloom", *Geophys. Res. Lett.* **29** (2002) 1534–1537; doi:10.1029/2001GL013677.

[17] PDE Solutions Inc., FlexPDE, 2014; http://www.pdesolutions.com.
[18] W. E. Ranz, "Applications of a stretch model to mixing, diffusion, and reaction in laminar and turbulent flows", *AIChE J.* **25** (1979) 41–47; doi:10.1002/aic.690250105.
[19] W. E. Schiesser, *The numerical method of lines: integration of partial differential equations* (Academic Press, San Diego, CA, 1991).
[20] J. J. Sharples, H. S. Sidhu, A. C. McIntosh, J. Brindley and V. V. Gubernov, "Analysis of combustion waves arising in the presence of a competitive endothermic reaction", *IMA J. Appl. Math.* **77** (2012) 18–31; doi:10.1093/imamat/hxr072.
[21] V. P. Sinditskii, V. Y. Egorshev, A. I. Levshenkov and V. V. Serushkin, "Ammonium nitrate: combustion mechanism and the role of additives", *Propellants Explosives Pyrotech.* **30** (2005) 269–280; doi:10.1002/prep.200500017.
[22] T. Tel, A. de Moura, C. Grebogi and G. Karolyi, "Chemical and biological activity in open flows: a dynamical systems approach", *Phys. Rep.* **413** (2005) 91–196; doi:10.1016/j.physrep.2005.01.005.
[23] R. Turcotte, S. Goldthorpe, C. M. Badeem, H. Feng and S. K. Chan, "Influence of physical characteristics and ingredients on the minimum burning pressure of ammonium nitrate emulsions", *Propellants Explosives Pyrotech.* **35** (2010) 233–239; doi:10.1002/prep.201000019.
[24] Y. B. Zeldovich, G. I. Barenblatt, V. B. Librovich and G. M. Makhviladze, *The mathematical theory of combustion and explosions* (Consultants Bureau, New York, 1985); doi:10.1007/978-1-4613-2349-5.